THE JOURNAL OF PHYSICAL CHEMISTRY LETTERS
A JOURNAL OF THE AMERICAN CHEMICAL SOCIETY

pubs.acs.org/JPCL Letter

Unexpected Photodriven Linker-to-Node Hole Transfer in a Zirconium-Based Metal−Organic Framework

Boris V. Kramar, Anna S. Bondarenko, Sydney M. Koehne, Benjamin T. Diroll, Xiaodan Wang, Haofan Yang, Kirk S. Schanze, Lin X. Chen,* Roel Tempelaar,* and Joseph T. Hupp*

Cite This: J. Phys. Chem. Lett. 2024, 15, 11496−11503 Read Online

ACCESS | Metrics & More | Article Recommendations | Supporting Information

ABSTRACT: $Zr_6(\mu_3\text{-}O)_4(\mu_3\text{-}OH)_4$ node cores are indispensable building blocks for almost all zirconium-based metal−organic frameworks. Consistent with the insulating nature of zirconia, they are generally considered electronically inert. Contrasting this viewpoint, we present spectral measurements and calculations indicating that emission from photoexcited NU-601, a six-connected Zr-based MOF, comes from both linker-centric locally excited and linker-to-node charge-transfer (CT) states. The CT state originates from a hole transfer process enabled by favorable energy alignment of the HOMOs of the node and linker. This alignment can be manipulated by changing the pH of the medium, which alters the protonation state of multiple oxy groups on the Zr-node. Thus, the acid−base chemistry of the node has a direct effect on the photophysics of the MOF following linker-localized electronic excitation. These new findings open opportunities to understand and exploit, for energy conversion, unconventional mechanisms of exciton formation and transport in MOFs.

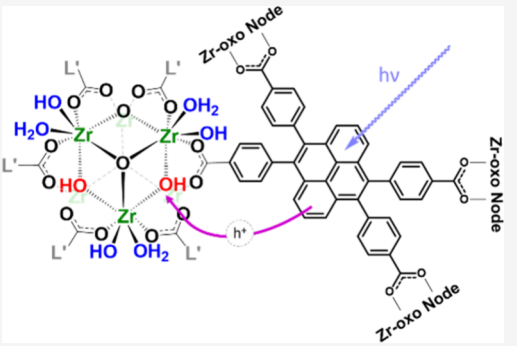

Zirconium-based metal−organic frameworks (Zr-MOFs) are promising light-harvesting platforms due to their high porosity, stability, and topological variety,[1−10] as well as their ability to organize chromophores (organic linkers) for extended, directional transport of photogenerated molecular excitons. In favorable instances, hundreds of linkers can be enlisted for propagation of a single exciton, collections of linkers can function as antennae, and, via terminal exciton splitting, frameworks can deliver oxidizing or reducing equivalents to sites far removed from the point of optical excitation.[11−15] Notably, if the sites are coupled to catalysts or electrodes, photonic energy can, in principle, be converted to stored chemical or useable electrical energy.[16]

Importantly, a widely used node core for Zr-MOFs, $Zr_6(\mu_3\text{-}O)_4(\mu_3\text{−}OH)_4^{12+}$, is believed, based on the large and unfavorably positioned optical gap of ZrO_2,[17,18] to be optoelectronically inert. Having zero valence electrons, Zr(IV) cannot be chemically oxidized. Furthermore, apart from high-temperature reaction of zirconia with H_2 to form lattice oxygen vacancies and water vapor,[19] chemical reduction of Zr(IV) in oxy ligand environments is almost never encountered.

The redox-inert nature of oxy-Zr(IV) species prevents unwanted redox-quenching of photogenerated excited-states, while also ensuring that frameworks are not disrupted by reduction-engendered weakening of metal (node)/oxy-anion (linker) bonds or restructuring of coordination motifs. Additionally, Truhlar et al. and others have shown computationally that photodriven (visible or near-UV) linker-to-zirconium electron-transfer, is, in general, energetically unfavorable,[18,20,21] and Patwardhan et al. have shown that electronic-coupling-controlled, redox-hopping between linkers can be well understood by altogether neglecting Zr(IV).[22]

Given the apparent redox-innocence of Zr(IV) and the seeming electronic energetic misalignment of linkers and nodes, we were surprised to find that fluorescence of the Zr-MOF, NU-601 (Scheme 1, Figure S1), following linker-localized photoexcitation, is strongly dependent on the extent of "inert" node protonation. Indeed, both the fluorescence intensity and line shape change drastically, but reversibly, with solution pH. Experiments and computations reveal intense, pH-tunable photoemission from a rapidly formed, but indirectly populated linker-to-node charge-transfer (CT) state. The transferred charge, however, is a hole rather than an electron, and the charge acceptor is an oxygenic, rather than metal-ion, component of the node. While not developed here, the prevalence of this unusual excited-state could have profound mechanistic implications for energy transport and antenna behavior in photoactive Zr-MOFs.

NU-601 is a six-connected MOF containing pyrene-derived linkers.[23] The experimental absorption spectrum of the

Received: September 30, 2024
Revised: October 27, 2024
Accepted: October 29, 2024
Published: November 8, 2024

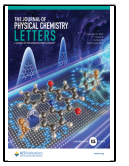

Scheme 1. Structure of NU-601 (a);[23] Zr Node Shown from c-axis: All Six Linker Connections and Half the Core and Nonstructural Oxygenic Ligands (b); L′ Represents the Rest of the Linker (c); Each Linker Connects to Four Nodes

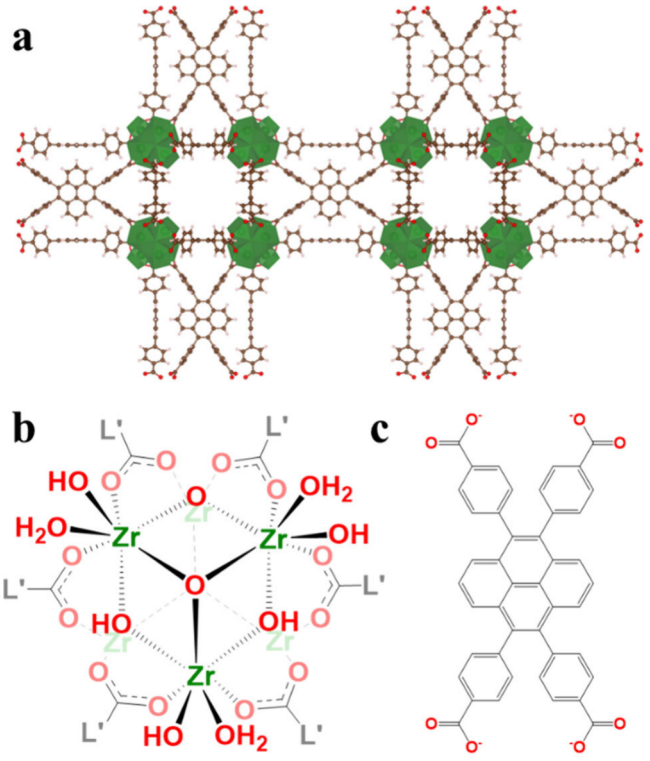

solubilized linker (Figure 1) features a weak transition at ∼3.27 eV (370 nm, highlighted), located below the principal transition at 3.55 eV. Time-dependent density-functional-theory (TD-DFT) calculations (SI Section S3) associate this weak transition with a transition dipole along the long axis of the pyrene. No Stokes shift is observed between the lowest energy absorption band and the 0−0 fluorescence peak. We anticipated that NU-601 would display similar emission, since its nearest-neighbor linkers/chromophores: 1) are separated by Zr-nodes or by pores with center-to-center distances >10 Å, and 2) possess transition dipoles oriented 90° with respect to each other. Notably, these structural features should largely preclude both linker-to-linker resonance energy transfer and excimer formation.[24,4,25] NU-601's emission maximum (in DMF) is ∼2.97 eV. At first glance, this seems to constitute a 0.30 eV bathochromic shift compared to the linker fluorescence spectrum. Closer inspection shows, however, that the 3.27 eV band is preserved in both the absorption and emission spectra of the MOF. The experimental absorption spectrum of the MOF is largely featureless, owing to the nature of diffuse-reflectance measurement; for this reason, absorption spectrum computation was not performed.

We modeled all spectra based on a vibronic transition model, parametrized against *ab initio* calculations and experimental data (SI Section S3). TD-DFT calculations of the linker show that the principal transition at 3.55 eV is dominated by a HOMO to LUMO+3 transition, while the transition corresponding to the direct HOMO−LUMO gap possesses much less oscillator strength. Replication of the dominant MOF emission feature at 2.97 eV alongside the observable HOMO−LUMO linker absorption requires inclusion of an emitting state consistent with an indirectly formed linker-to-node CT state. Although not explored, previous computational work for the Zr-MOF UiO-66 (featuring a chemically related linker) showed a proximal energy alignment between linker and node HOMOs, making linker*-to-node hole transfer (Figure 1c) plausible.[18] (Linker* denotes photoexcited linker.)

Based on our spectral analysis, we posit linker*-to-node hole transfer in NU-601 giving rise to a CT state emitting at 2.97 eV, with a 0.30 eV redshift relative to the HOMO−LUMO transition in the linker-centered excitation, henceforth referred to as locally excited (LE) state (Figure 1c). The conduction band-edge energy of ZrO_2 (used to approximate node LUMO) lies very high on an absolute energy scale, ruling out electron transfer from photoexcited linkers to Zr-nodes to yield Zr(III) (SI Section S3). *Hole* transfer, however, has seen little

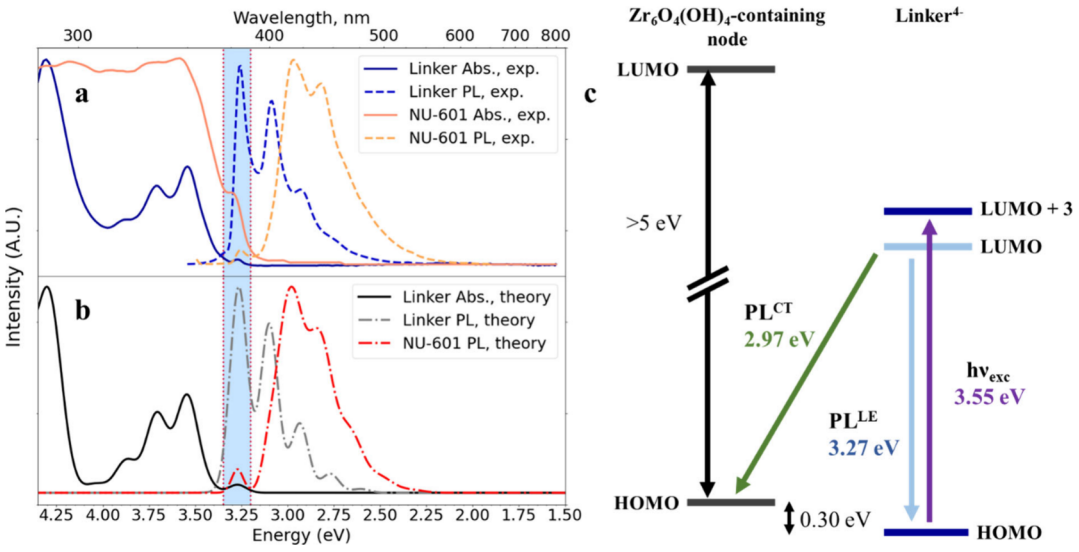

Figure 1. Experimental (a) and theoretical (b) absorption and emission spectra of NU-601 and its linker in dimethylformide (DMF); (c) the energy diagram shows the relevant transitions: HOMO → LUMO+3 is the dominant contributor to the principal transition at 3.55 eV. The HOMO−LUMO gap of the oxy-Zr node is assumed to exceed 5 eV.[26]

https://doi.org/10.1021/acs.jpclett.4c02848
J. Phys. Chem. Lett. 2024, 15, 11496−11503

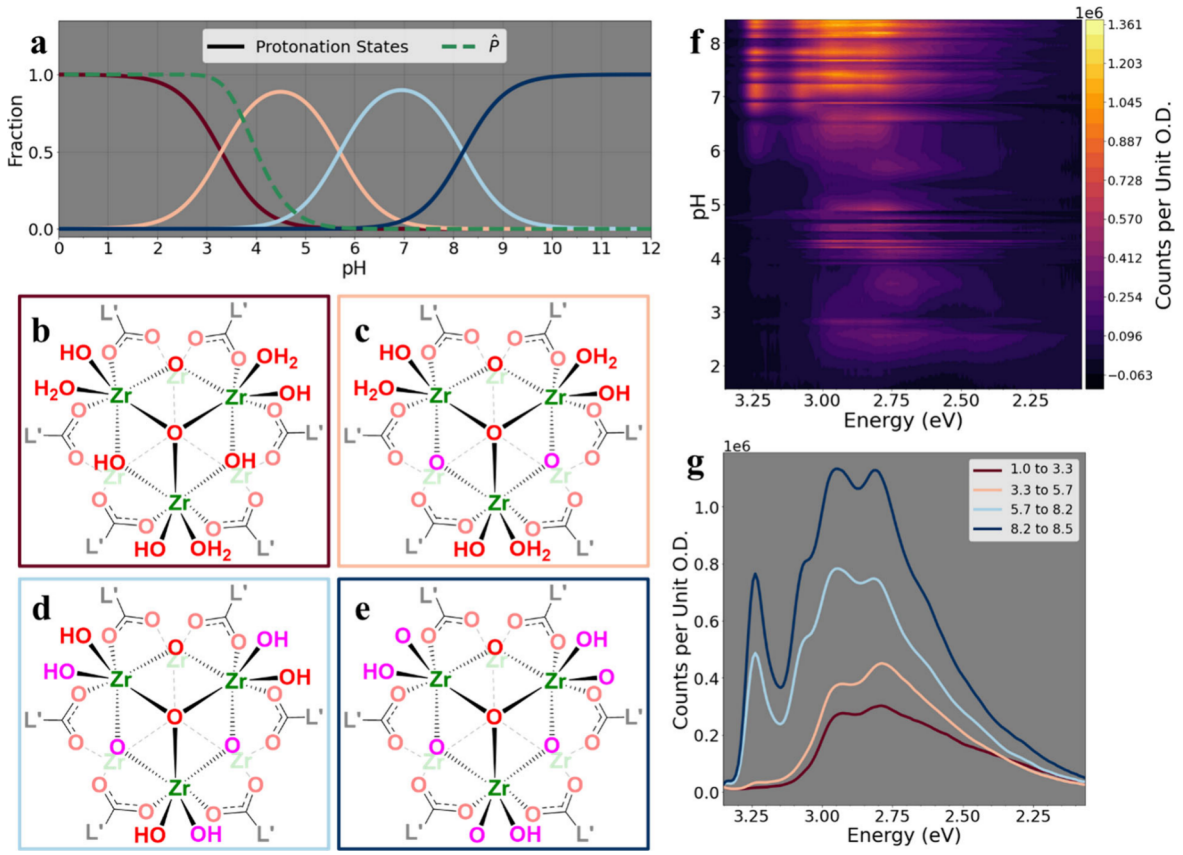

Figure 2. (a) Distribution of various node protonation states as a function of pH, based on the pK_a values reported by Klet et al.[40] $\hat{P}$ represents the probability of having at least one of four tetratopic-linker-connected nodes with a bridging-hydroxo proton still in place; see SI Section S2. (b–e) Schematic depictions of the Zr node, shown with all six linkers and half of the node's oxygenic groups. Schemes are arranged to show successive deprotonation. Emission as a function of pH is pooled in the contour plot (f) and binned along the pH axis into bins defined by pK_a values (g). Curves in a and g and outlines in b–e are color-coded.

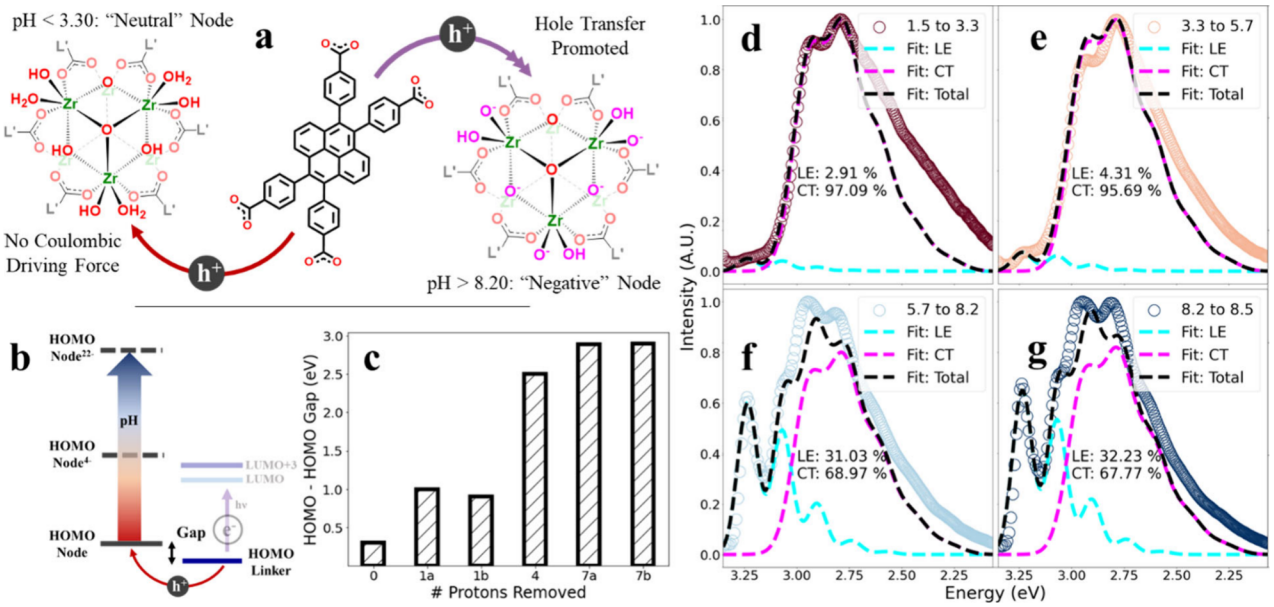

Figure 3. Schematic representation of the Coulombic argument in linker*-to-node hole transfer (a), the effect of deprotonation on the node HOMO level (b) and the resulting computed HOMO–HOMO gap (c), and linear combination fitting of compound pH-dependent fluorescence spectrum to the computed LE and CT state contributions (d–g).

discussion (apart from through-space transfer to node-*appended* metal-ions or molecules).[8,11,27,28] We propose that the CT state forms as a state spectrally distinct from the LE state, but with both contributing to the total emission

https://doi.org/10.1021/acs.jpclett.4c02848
J. Phys. Chem. Lett. 2024, 15, 11496–11503

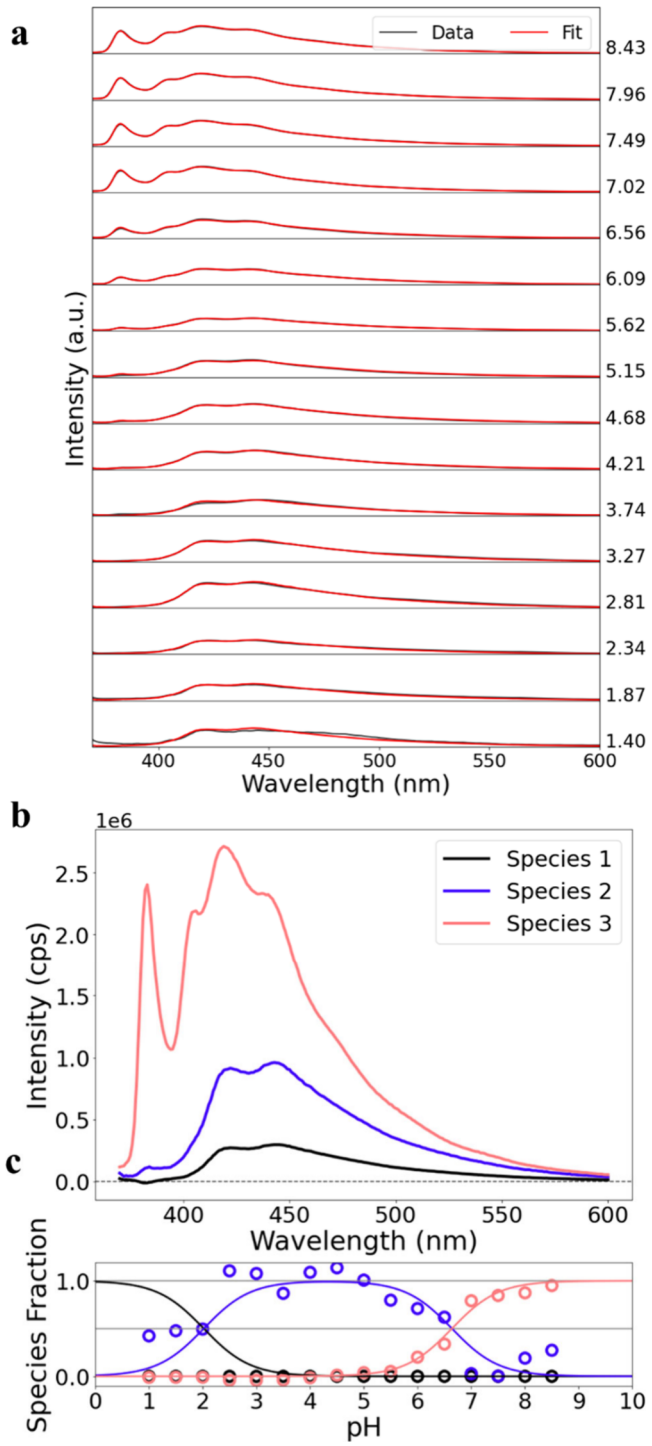

Figure 4. Fluorescence spectra (a) from Figure 2f rebinned with respect to pH, plotted with fits described by (b) species-associated spectra extracted via global fitting to Henderson–Hasselbalch equations, and (c) the corresponding species-associated populations versus pH.

spectrum.[29] Moreover, the CT state evolves from the LE state and is facilitated by the donor–acceptor like local structure within the MOF, with excited linkers serving as hole donors and nodes as hole acceptors.[30,31]

To further substantiate the CT state assignment, we consider variations in the solvent environment. Changes in the dielectric constant and/or viscosity[32,33] of the framework-permeating solvent engender only slight changes in the energy of the excited state (SI Figures S5 and S6). In contrast, varying the pH of the aqueous medium in the 1.5 to 8.5 range led to a pronounced modulation of the emission line shape and overall quantum yield, particularly that of the linker-based HOMO–LUMO emission band, consistent with populations of both CT and LE states being pH-dependent (Figure 2f,g). Similar, but subtler effects are observed in methanol (Figure S7a). Moreover, when photoluminescence measurements are performed in a nonpolar solvent but in the presence of either electron-donating (acetylacetonato) or electron-withdrawing (hexafluoroacetylacetonato) ligands known to coordinate with the zirconium node,[34,35] the LE and CT populations also change (SI Section S12). The experiment also revealed an apparent shift in the emission maximum of the CT state, which is likely to reflect either a rebalance in the vibronic transitions composing this emission band, or a change in E_{00} due to a change in energy of the hole-accepting orbital. Clearly, the extent of CT state formation is connected to the protonation state of the node.

Transient fluorescence studies (SI Section S11) show that the overall emissive state lifetime varies from about 20 ns at near-neutral pH to about 5 ns in a highly acidic environment, and spectral evolution is consistent with what is observed in the steady state. It is tempting to ascribe lifetime attenuation in acid to participation of μ_3–O-H stretches as high-frequency energy acceptors for nonradiative decay–an influence that ought to be present only if hole-transfer to hydroxo-bearing nodes occurs.[36,37]

To better understand pH influences, consider the $Zr_6O_4(OH)_4$-containing node in a modulator- and formate-free Zr-MOF.[38] Below the maximum connectivity of 12,[39] sites that would otherwise be occupied by linker-terminating carboxylates instead feature nonstructural hydroxo and aqua ligands in equal numbers. The oxygen sites present are bridging oxo, bridging hydroxo, terminal hydroxo, terminal aqua, and carboxylate. Three of these five carry protons (Scheme 1b). Notably, pK_a values for the protonated sites, on Zr-MOF nodes, have previously been determined.[40−42] The presence of multiple distinct pK_a values means that the node can be treated as a polyprotic acid. The Henderson–Hasselbalch equations can be used to obtain populations of various deprotonated node species as a function of pH (Figure 2a–e).[43] We use 3.3, 5.7, and 8.2 as pK_a estimates for NU-601; these values are representative across a range of Zr-MOFs.[40−42] In relating CT state formation to node protonation, we consider both average bulk populations and the probability of finding at least one of four linker-connected nodes in a given protonation state (Figure 2a). Neglected is another pK_a, likely <1, corresponding to conditions where six terminal hydroxos have been converted to six additional $-OH_2$ ligands.[38]

We suggest two main effects that drive the pH dependence of the excited-state properties: (1) the Coulombic interactions that should promote linker*-to-node hole transfer based on charge changes upon node deprotonation (Figure 3a); and (2) the rise of the HOMO energy level of the node with deprotonation shown by our TD-DFT calculations, implying that deprotonation of the node breaks the linker-node orbital energy alignment and shifts the LE/CT excited-state distribution (Figure 3b). In fact, our calculations show a large increase in the HOMO–HOMO energy gap — albeit, with only an approximate estimate since the calculated cluster

https://doi.org/10.1021/acs.jpclett.4c02848
J. Phys. Chem. Lett. 2024, 15, 11496−11503

Scheme 2. Summary of the CT Exciton Formation Mechanism

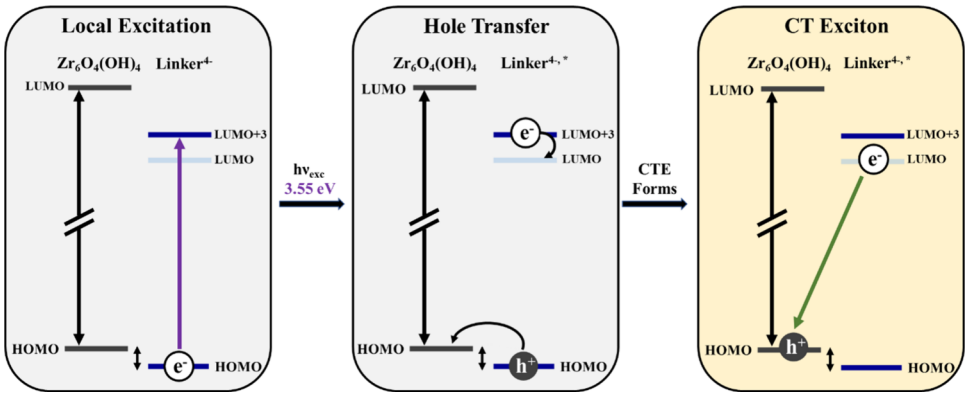

comprises one node with six benzoate "caps" instead of full linkers (Figure 3c and SI Section S3). Linear combination fitting (LCF) (Figure 3d−g) of pH-binned spectra to theoretical LE and CT fluorescence lineshapes captures the appearance of the LE contribution, but also clearly shows that the CT contribution is dominant regardless of pH, in contrast to the populations predicted by acid equilibrium (Figure 2a). This implies that multiple physical effects are relevant and that neither of the arguments can be taken in isolation. At the simplest level, linker*-to-node CT state formation is pairwise; thus, we suggest that the persistence of the CT state across the entire pH range may be explained by the fact that a linker can always find a node to which it can transfer a hole. The probability of a linker being connected to at least one node with a μ_3-O**H** protons still in place falls to 1% at about pH 6.4 (Figure 2a); both linker-to-linker exciton hopping and dynamic protonation presumably would increase the likelihood of an encounter between an LE-type exciton and a protonated node, and extend the pH range.[44] Additionally, the 33% share of the LE contribution observed at high pH appears to be consistent with the 1:1.5 node-linker stoichiometry in NU-601; assuming similar quantum yields, we can hypothesize that at high pH CT state population is saturated.

Since LCF was insufficient to reconstruct emission signatures as a function of pH, we turned to principal component analysis (PCA). This method decomposes the observed data into multiple best-fit contributors. The optimal number of contributors can be determined via singular value decomposition (SI Section S10). Ratios of contributions vary with pH. Consequently, the Henderson−Hasselbalch equations can be used as a mechanistic model to guide PCA. Within the routine, pK_a values are allowed to vary; since fluorescence reports on excited states, the best fit pK_a values here must correspond to excited-state pK_a values, pK_a* (for additional discussion, see SI Section S2). In the specific case of hole transfer to the node, we expect at least one pK_a* value to decrease compared to ground-state pK_a due to net increase in positive charge on the node. PCA results are shown in Figure 4b and 4c. We fit data to three components (two pK_a* values), because this is sufficient to describe the data (see Figure S10). The analysis returns pK_a* values of 2.0 and 6.6 with negligible fitting uncertainties.

Typically, K_a* for a photoacid will be higher than that for the ground state K_a by several orders of magnitude,[45,46] although smaller changes−i.e., $\Delta pK_a \approx 1$−are not uncommon.[47] While three pK_as have been measured for the node in the ground state, only two are necessary to describe the excited state. We infer that the pK_a* of 2.0 corresponds to the ground state pK_a of 3.3, reflecting the increased acidity of μ_3-hydroxos upon hole injection. There is a concurrent decrease in acidity of aqua ligands from GS pK_a = 5.8 to pK_a*=6.6.

Experimental emission spectra and accompanying theory work evince communication between LE and CT states, where the charge-transfer state is formed by linker*-to-node hole transfer (Scheme 2). This notion is substantiated by node protonation influencing emission despite the node not being part of the absorbing chromophore. (It is conceivable that at a high enough pH, the HOMO−HOMO energy gap changes sign and direct node-to-linker electron transfer becomes possible; however, such ground-state charge-transfer species could be susceptible to rapid recombination or an annihilation reaction with triplet oxygen). However, the high-pH spectral contributor (Figure 4b, Species 3) extracted through target analysis does not perfectly match the theoretical LE line shape from Figure 3d-g, suggesting that the high-pH component is a mix of LE and CT states. This picture is consistent with the presented explanation of electronic effects (node HOMO level affected by pH) in competition with Coulombic effects (diminished positive charge on the node core promoting hole transfer). The presence of solvent electrolyte was also found to have an effect; the CT state may be stabilized at a higher pH by compensating the missing protons with alkali metal cations (see Figure S8).

The presence of the CT state has important implications for Zr-MOFs in photochemical applications, especially those involving/requiring antenna behavior and long-range energy transport. As an alternative to FRET (Förster resonance energy transfer),[48] the CT state may offer a basis for energy transport via an unconventional superexchange mechanism, first described by Haarer et al., where LE states facilitate charge-carrier tunneling.[30,49] While the orthogonal positioning of nearest-neighbor lowest energy transition dipoles in NU-601 likely precludes this framework from efficiently transporting energy via FRET, this superexchange mechanism could plausibly give rise to significant exciton mobilities.

More broadly, our work shows that the optoelectronic properties of selected Zr-MOFs are dependent on formation of CT states or excitons, as opposed to the LE-dominated behavior observed in MOFs such as NH_2-MIL-53 and ZIF-67.[50,51] Clearly, NU-601 with its UV-centric absorption band is not a particularly promising light-harvesting system, even if it is capable of performing basic photochemistry (see SI Section S9). However, having demonstrated that the electronic properties of the material can be tuned by (de)protonating

https://doi.org/10.1021/acs.jpclett.4c02848
J. Phys. Chem. Lett. 2024, 15, 11496−11503

the node due to the partial charge-transfer character of the excited state, we posit that this study carries important implications for the enduring question of long-range energy transport mechanisms in Zr-MOFs. We speculate that the reported fluorescence sensitivity of NU-1000 to cyanide-containing solutions is a manifestation of tuning of an emissive linker*-to-node CT state, like that explored here for NU-601.[52] We further suggest that the unusually large fluorescence Stokes shift for NU-1000 reflects emission from a different state (linker*-to-node hole-transfer) than the one created by absorption (linker-localized excitation).[9] Closely related may be the ability of NU-1000 to propagate photogenerated excitons across hundreds of linkers, despite minimal overlap of absorption and fluorescence spectra.[11] If energy transport is accomplished by the above-mentioned, CT-enabled Haarer-superexchange mechanism, rather than FRET, such overlap would not be needed. The presence of the CT state, and the ability to tune the dynamics of its formation, also allows for resonance energy transport (when present) to be tuned at will by altering the local pH at the Zr-oxo node. Protonation state does not have to be the only method to achieve such tuning; changes like introducing formate caps may achieve the same goal.[53] Assessment of the potential quantitative applicability of the CT-enabled scheme to long-range energy transport within selected Zr-MOFs is a focus of ongoing work.

EXPERIMENTAL METHODS

The experimental methods are described in the Supporting Information.

ASSOCIATED CONTENT

Supporting Information

The Supporting Information is available free of charge at https://pubs.acs.org/doi/10.1021/acs.jpclett.4c02848.

> Experimental methods (synthesis, data collection, data treatment, theory); nuclear magnetic resonance (NMR) spectra; powder X-ray diffraction (PXRD) data; N_2 sorption data; additional sets of emission data in different solvent environments; SEM images; FLIM images; experiments with methyl viologen; time-resolved emission; and additional discussion (PDF)

AUTHOR INFORMATION

Corresponding Authors

Lin X. Chen − *Department of Chemistry, Northwestern University, Evanston, Illinois 60208, United States; Chemical Sciences and Engineering Division, Argonne National Laboratory, Argonne, Illinois 60439, United States;* orcid.org/0000-0002-8450-6687; Email: l-chen@northwestern.edu, lchen@anl.gov

Roel Tempelaar − *Department of Chemistry, Northwestern University, Evanston, Illinois 60208, United States;* orcid.org/0000-0003-0786-7304; Email: roel.tempelaar@northwestern.edu

Joseph T. Hupp − *Department of Chemistry, Northwestern University, Evanston, Illinois 60208, United States;* orcid.org/0000-0003-3982-9812; Email: j-hupp@northwestern.edu

Authors

Boris V. Kramar − *Department of Chemistry, Northwestern University, Evanston, Illinois 60208, United States;* orcid.org/0000-0001-8731-7542

Anna S. Bondarenko − *Department of Chemistry, Northwestern University, Evanston, Illinois 60208, United States*

Sydney M. Koehne − *Department of Chemistry, Northwestern University, Evanston, Illinois 60208, United States;* orcid.org/0000-0001-8662-572X

Benjamin T. Diroll − *Nanoscience and Technology Division, Argonne National Laboratory, Argonne, Illinois 60439, United States;* orcid.org/0000-0003-3488-0213

Xiaodan Wang − *Department of Chemistry, University of Texas at San Antonio, San Antonio, Texas 78249, United States;* orcid.org/0009-0006-3799-950X

Haofan Yang − *Department of Chemistry, Northwestern University, Evanston, Illinois 60208, United States;* orcid.org/0000-0002-1338-7705

Kirk S. Schanze − *Department of Chemistry, University of Texas at San Antonio, San Antonio, Texas 78249, United States;* orcid.org/0000-0003-3342-4080

Complete contact information is available at: https://pubs.acs.org/10.1021/acs.jpclett.4c02848

Notes

The authors declare no competing financial interest.
MOFkey: Zr. MWVMNBLQHRBBOY. MOFkey-v1.she (NU-601)[54]

ACKNOWLEDGMENTS

J.T.H. gratefully acknowledges support from the U.S. Dept. of Energy, Office of Science, Basic Energy Sciences, Solar Photochemistry Program (grant number DE-FG02-87ER13808). Work performed at the Center for Nanoscale Materials, a U.S. Department of Energy Office of Science User Facility, was supported by the U.S. DOE, Office of Basic Energy Sciences, under Contract No. DE-AC02-06CH11357. A.S.B. and R.T. acknowledge support from the National Science Foundation under Grant No. CHE-2145433. B.V.K. is partially supported by a MURI Grant from ONR (N00014-20-1-2517) to L.X.C. The effort of L.X.C. is partially supported by the U.S. Department of Energy, Office of Science, Office of Basic Energy Sciences, under Contract No. DE-AC02-06CH11357.

REFERENCES

(1) Wang, J.-L.; Wang, C.; Lin, W. Metal−Organic Frameworks for Light Harvesting and Photocatalysis. *ACS Catal.* **2012**, *2* (12), 2630−2640.

(2) Benseghir, Y.; Solé-Daura, A.; Cairnie, D. R.; Robinson, A. L.; Duguet, M.; Mialane, P.; Gairola, P.; Gomez-Mingot, M.; Fontecave, M.; Iovan, D.; et al. Unveiling the mechanism of the photocatalytic reduction of CO2to formate promoted by porphyrinic Zr-based metal−organic frameworks. *Journal of Materials Chemistry A* **2022**, *10* (35), 18103−18115.

(3) Shaikh, S. M.; Chakraborty, A.; Alatis, J.; Cai, M.; Danilov, E.; Morris, A. J. Light harvesting and energy transfer in a porphyrin-based metal organic framework. *Faraday Discuss.* **2019**, *216*, 174−190.

(4) Shaikh, S. M.; Ilic, S.; Gibbons, B. J.; Yang, X.; Jakubikova, E.; Morris, A. J. Role of a 3D Structure in Energy Transfer in Mixed-Ligand Metal−Organic Frameworks. *J. Phys. Chem. C* **2021**, *125* (42), 22998−23010.

(5) Shaikh, S. M.; Usov, P. M.; Zhu, J.; Cai, M.; Alatis, J.; Morris, A. J. Synthesis and Defect Characterization of Phase-Pure Zr-MOFs Based on Meso-tetracarboxyphenylporphyrin. *Inorg. Chem.* **2019**, *58* (8), 5145−5153.
(6) Deria, P.; Yu, J.; Balaraman, R. P.; Mashni, J.; White, S. N. Topology-dependent emissive properties of zirconium-based porphyrin MOFs. *Chem. Commun. (Camb)* **2016**, *52* (88), 13031−13034.
(7) Deria, P.; Yu, J.; Smith, T.; Balaraman, R. P. Ground-State versus Excited-State Interchromophoric Interaction: Topology Dependent Excimer Contribution in Metal-Organic Framework Photophysics. *J. Am. Chem. Soc.* **2017**, *139* (16), 5973−5983.
(8) Li, X.; Yu, J.; Gosztola, D. J.; Fry, H. C.; Deria, P. Wavelength-Dependent Energy and Charge Transfer in MOF: A Step toward Artificial Porous Light-Harvesting System. *J. Am. Chem. Soc.* **2019**, *141* (42), 16849−16857.
(9) Rajasree, S. S.; Yu, J.; Pratik, S. M.; Li, X.; Wang, R.; Kumbhar, A. S.; Goswami, S.; Cramer, C. J.; Deria, P. Superradiance and Directional Exciton Migration in Metal−Organic Frameworks. *J. Am. Chem. Soc.* **2022**, *144* (3), 1396−1406.
(10) Yu, J.; Li, X.; Deria, P. Light-Harvesting in Porous Crystalline Compositions: Where We Stand toward Robust Metal−Organic Frameworks. *ACS Sustainable Chem. Eng.* **2019**, *7* (2), 1841−1854.
(11) Goswami, S.; Yu, J.; Patwardhan, S.; Deria, P.; Hupp, J. T. Light-Harvesting "Antenna" Behavior in NU-1000. *ACS Energy Letters* **2021**, *6* (3), 848−853.
(12) Kumagai, K.; Uematsu, T.; Torimoto, T.; Kuwabata, S. Photoluminescence Enhancement by Light Harvesting of Metal−Organic Frameworks Surrounding Semiconductor Quantum Dots. *Chem. Mater.* **2021**, *33* (5), 1607−1617.
(13) Van Wyk, A.; Smith, T.; Park, J.; Deria, P. Charge-Transfer within Zr-Based Metal-Organic Framework: The Role of Polar Node. *J. Am. Chem. Soc.* **2018**, *140* (8), 2756−2760.
(14) Liu, L.; Lu, X.-Y.; Zhang, M.-L.; Ren, Y.-X.; Wang, J.-J.; Yang, X.-G. 2D MOF nanosheets as an artificial light-harvesting system with enhanced photoelectric switching performance. *Inorganic Chemistry Frontiers* **2022**, *9* (11), 2676−2682.
(15) Afrin, S.; Yang, X.; Morris, A. J.; Grumstrup, E. M. Rapid Exciton Transport and Structural Defects in Individual Porphyrinic Metal Organic Framework Microcrystals. *J. Am. Chem. Soc.* **2024**, *146* (7), 4309−4313.
(16) Patel, J.; Bury, G.; Pushkar, Y. Rational Design of Improved Ru Containing Fe-Based Metal-Organic Framework (MOF) Photoanode for Artificial Photosynthesis. *Small* **2024**, *20* (37), No. 2310106.
(17) Gionco, C.; Paganini, M. C.; Giamello, E.; Burgess, R.; Di Valentin, C.; Pacchioni, G. Cerium-Doped Zirconium Dioxide, a Visible-Light-Sensitive Photoactive Material of Third Generation. *J. Phys. Chem. Lett.* **2014**, *5* (3), 447−451.
(18) Wu, X.-P.; Gagliardi, L.; Truhlar, D. G. Cerium Metal−Organic Framework for Photocatalysis. *J. Am. Chem. Soc.* **2018**, *140* (25), 7904−7912.
(19) Eder, D.; Kramer, R. The stoichiometry of hydrogen reduced zirconia and its influence on catalytic activity. *Phys. Chem. Chem. Phys.* **2002**, *4* (5), 795−801.
(20) Nasalevich, M. A.; Hendon, C. H.; Santaclara, J. G.; Svane, K.; van der Linden, B.; Veber, S. L.; Fedin, M. V.; Houtepen, A. J.; van der Veen, M. A.; Kapteijn, F.; et al. Electronic origins of photocatalytic activity in d0 metal organic frameworks. *Sci. Rep.* **2016**, *6* (1), 23676.
(21) Hendrickx, K.; Vanpoucke, D. E. P.; Leus, K.; Lejaeghere, K.; Van Yperen-De Deyne, A.; Van Speybroeck, V.; Van Der Voort, P.; Hemelsoet, K. Understanding Intrinsic Light Absorption Properties of UiO-66 Frameworks: A Combined Theoretical and Experimental Study. *Inorg. Chem.* **2015**, *54* (22), 10701−10710.
(22) Patwardhan, S.; Schatz, G. C. Theoretical Investigation of Charge Transfer in Metal Organic Frameworks for Electrochemical Device Applications. *J. Phys. Chem. C* **2015**, *119* (43), 24238−24247.
(23) Lu, Z.; Wang, R.; Liao, Y.; Farha, O. K.; Bi, W.; Sheridan, T. R.; Zhang, K.; Duan, J.; Liu, J.; Hupp, J. T. Isomer of linker for NU-1000 yields a new she-type, catalytic, and hierarchically porous, Zr-based metal-organic framework. *Chem. Commun. (Camb)* **2021**, *57* (29), 3571−3574.
(24) Wan, R.; Ha, D. G.; Dou, J. H.; Lee, W. S.; Chen, T.; Oppenheim, J. J.; Li, J.; Tisdale, W. A.; Dinca, M. Dipole-mediated exciton management strategy enabled by reticular chemistry. *Chem. Sci.* **2022**, *13* (36), 10792−10797.
(25) Birks, J. B. Excimers. *Rep. Prog. Phys.* **1975**, *38* (8), 903.
(26) Emeline, A.; Kataeva, G. V.; Litke, A. S.; Rudakova, A. V.; Ryabchuk, V. K.; Serpone, N. Spectroscopic and Photoluminescence Studies of a Wide Band Gap Insulating Material: Powdered and Colloidal ZrO2 Sols. *Langmuir* **1998**, *14* (18), 5011−5022.
(27) Kramar, B. V.; Flanders, N. C.; Helweh, W.; Dichtel, W. R.; Hupp, J. T.; Chen, L. X. Light Harvesting Antenna Properties of Framework Solids. *Accounts of Materials Research* **2022**, *3* (11), 1149−1159.
(28) Li, Q.; Li, D.; Wu, Z.-Q.; Shi, K.; Liu, T.-H.; Yin, H.-Y.; Cai, X.-B.; Fan, Z.-L.; Zhu, W.; Xue, D.-X. RhB-Embedded Zirconium−Biquinoline-Based MOF Composite for Highly Sensitive Probing Cr(VI) and Photochemical Removal of CrO42−, Cr2O72−, and MO. *Inorg. Chem.* **2022**, *61* (38), 15213−15224.
(29) Qian, G.; Dai, B.; Luo, M.; Yu, D.; Zhan, J.; Zhang, Z.; Ma, D.; Wang, Z. Y. Band Gap Tunable, Donor−Acceptor−Donor Charge-Transfer Heteroquinoid-Based Chromophores: Near Infrared Photoluminescence and Electroluminescence. *Chem. Mater.* **2008**, *20* (19), 6208−6216.
(30) Haarer, D.; Philpott, M. R.; Morawitz, H. Field induced charge-transfer exciton transitions. *J. Chem. Phys.* **1975**, *63* (12), 5238−5245.
(31) Agranovich, V. M. *Excitations in Organic Solids*; Oxford University Press, 2008.
(32) Sasaki, S.; Drummen, G. P. C.; Konishi, G.-i. Recent advances in twisted intramolecular charge transfer (TICT) fluorescence and related phenomena in materials chemistry. *Journal of Materials Chemistry C* **2016**, *4* (14), 2731−2743.
(33) Yu, J.; Park, J.; Van Wyk, A.; Rumbles, G.; Deria, P. Excited-State Electronic Properties in Zr-Based Metal−Organic Frameworks as a Function of a Topological Network. *J. Am. Chem. Soc.* **2018**, *140* (33), 10488−10496.
(34) Chen, Z.; Stroscio, G. D.; Liu, J.; Lu, Z.; Hupp, J. T.; Gagliardi, L.; Chapman, K. W. Node Distortion as a Tunable Mechanism for Negative Thermal Expansion in Metal−Organic Frameworks. *J. Am. Chem. Soc.* **2023**, *145* (1), 268−276.
(35) Liu, J.; Ye, J.; Li, Z.; Otake, K.-i.; Liao, Y.; Peters, A. W.; Noh, H.; Truhlar, D. G.; Gagliardi, L.; Cramer, C. J.; et al. Beyond the Active Site: Tuning the Activity and Selectivity of a Metal−Organic Framework-Supported Ni Catalyst for Ethylene Dimerization. *J. Am. Chem. Soc.* **2018**, *140* (36), 11174−11178.
(36) Palit, D. K.; Pal, H.; Mukherjee, T.; Mittal, J. P. Photodynamics of the S1 state of some hydroxy- and amino-substituted naphthoquinones and anthraquinones. *Journal of the Chemical Society, Faraday Transactions* **1990**, *86* (23), 3861−3869.
(37) Avouris, P.; Gelbart, W. M.; El-Sayed, M. A. Nonradiative electronic relaxation under collision-free conditions. *Chem. Rev.* **1977**, *77* (6), 793−833.
(38) Lu, Z.; Liu, J.; Zhang, X.; Liao, Y.; Wang, R.; Zhang, K.; Lyu, J.; Farha, O. K.; Hupp, J. T. Node-Accessible Zirconium MOFs. *J. Am. Chem. Soc.* **2020**, *142* (50), 21110−21121.
(39) Kaur, G.; Øien-Ødegaard, S.; Lazzarini, A.; Chavan, S. M.; Bordiga, S.; Lillerud, K. P.; Olsbye, U. Controlling the Synthesis of Metal−Organic Framework UiO-67 by Tuning Its Kinetic Driving Force. *Cryst. Growth Des.* **2019**, *19* (8), 4246−4251.
(40) Klet, R. C.; Liu, Y.; Wang, T. C.; Hupp, J. T.; Farha, O. K. Evaluation of Brønsted acidity and proton topology in Zr- and Hf-based metal−organic frameworks using potentiometric acid−base titration. *Journal of Materials Chemistry A* **2016**, *4* (4), 1479−1485.
(41) Liao, Y. *Investigation of Metal-Organic Frameworks in Chemical Separations and Catalysis*. Ph.D., Northwestern University, United States, Illinois, 2020.

https://doi.org/10.1021/acs.jpclett.4c02848
J. Phys. Chem. Lett. 2024, 15, 11496−11503

(42) Chen, H. Computational study of Brønsted acidity in the metal−organic framework UiO-66. *Chem. Phys. Lett.* **2022**, *800*, No. 139658.
(43) Po, H. N.; Senozan, N. M. The Henderson-Hasselbalch Equation: Its History and Limitations. *J. Chem. Educ.* **2001**, *78* (11), 1499.
(44) Halder, A.; Bain, D. C.; Oktawiec, J.; Addicoat, M. A.; Tsangari, S.; Fuentes-Rivera, J. J.; Pitt, T. A.; Musser, A. J.; Milner, P. J. Enhancing Dynamic Spectral Diffusion in Metal−Organic Frameworks through Defect Engineering. *J. Am. Chem. Soc.* **2023**, *145* (2), 1072−1082.
(45) Solntsev, K. M.; Huppert, D.; Tolbert, L. M.; Agmon, N. Solvatochromic shifts of″ super″ photoacids. *J. Am. Chem. Soc.* **1998**, *120* (31), 7981−7982.
(46) Spies, C.; Shomer, S.; Finkler, B.; Pines, D.; Pines, E.; Jung, G.; Huppert, D. Solvent dependence of excited-state proton transfer from pyranine-derived photoacids. *Phys. Chem. Chem. Phys.* **2014**, *16* (19), 9104−9114.
(47) Chakraborty, S.; Nandi, S.; Bhattacharyya, K.; Mukherjee, S. Time Evolution of Local pH Around a Photo-Acid in Water and a Polymer Hydrogel: Time Resolved Fluorescence Spectroscopy of Pyranine. *ChemPhysChem* **2019**, *20* (23), 3221−3227.
(48) Forster, T. Energiewanderung und fluoreszenz. *Naturwissenschaften* **1946**, *33* (6), 166−175.
(49) Schlesinger, I.; Powers-Riggs, N. E.; Logsdon, J. L.; Qi, Y.; Miller, S. A.; Tempelaar, R.; Young, R. M.; Wasielewski, M. R. Charge-transfer biexciton annihilation in a donor-acceptor co-crystal yields high-energy long-lived charge carriers. *Chem. Sci.* **2020**, *11* (35), 9532−9541.
(50) Hanna, L.; Kucheryavy, P.; Liu, C.; Zhang, X.; Lockard, J. V. Long-Lived Photoinduced Charge Separation in a Trinuclear Iron-μ3-oxo-based Metal-Organic Framework. *J. Phys. Chem. C* **2017**, *121* (25), 13570−13576.
(51) Hu, W.; Yang, F.; Pietraszak, N.; Gu, J.; Huang, J. Distance dependent energy transfer dynamics from a molecular donor to a zeolitic imidazolate framework acceptor. *Phys. Chem. Chem. Phys.* **2020**, *22* (44), 25445−25449.
(52) Luconi, L.; Mercuri, G.; Islamoglu, T.; Fermi, A.; Bergamini, G.; Giambastiani, G.; Rossin, A. Benzothiazolium-functionalized NU-1000: a versatile material for carbon dioxide adsorption and cyanide luminescence sensing. *Journal of Materials Chemistry C* **2020**, *8* (22), 7492−7500.
(53) Kramar, B. V. *The Relationship Between Node Ligand Environment and Excited State Dynamics of Zirconium-Based Metal—Organic Frameworks*. Ph.D. Disseration, Northwestern University, 2023.
(54) Bucior, B. J.; Rosen, A. S.; Haranczyk, M.; Yao, Z.; Ziebel, M. E.; Farha, O. K.; Hupp, J. T.; Siepmann, J. I.; Aspuru-Guzik, A.; Snurr, R. Q. Identification Schemes for Metal−Organic Frameworks To Enable Rapid Search and Cheminformatics Analysis. *Cryst. Growth Des.* **2019**, *19* (11), 6682−6697.

https://doi.org/10.1021/acs.jpclett.4c02848
J. Phys. Chem. Lett. 2024, 15, 11496−11503